

Effect of organic fuels on catalytic properties of $\text{La}_{0.8}\text{Sr}_{0.2}\text{CoO}_3$ with large surface area

Wei Liu, Laitao* & Yuehui Wu

Institute of Applied Chemistry, Nanchang University, Nanchang 330031, PR China
Email: luolaitao@163.com

Received 31 July 2007; revised 10 January 2008

Perovskite-type $\text{La}_{0.8}\text{Sr}_{0.2}\text{CoO}_3$ oxides have been prepared by solution combustion synthesis and their catalytic performance for CH_4 combustion reaction has been studied. The prepared samples have been characterized by XRD, IR, BET and TPR. The effect of organic fuels on the structure and the catalytic activities of $\text{La}_{0.8}\text{Sr}_{0.2}\text{CoO}_3$ catalysts have been investigated. Results indicate that all the $\text{La}_{0.8}\text{Sr}_{0.2}\text{CoO}_3$ catalysts prepared by solution combustion synthesis have large specific surface area, and the structure and catalytic activities of the catalysts are related to the organic fuels. The best catalytic activity is shown by the $\text{La}_{0.8}\text{Sr}_{0.2}\text{CoO}_3$ catalyst prepared with *DL*-alanine. The activity of the catalyst can be explained in terms of smaller crystallite size, larger specific surface area, lower activation energy and more mobility of chemisorbed oxygen on the surface and in the vacancies.

IPC Code: Int. Cl.⁸ B01J 21/00

Due to more stringent legislation concerning emissions of NO_x , CO and HC during the last two decades, catalytic combustion has emerged as a very promising technique for gas turbine applications. Several reviews published in this area clearly show the potential of this technique to achieve ultra-low levels of emissions¹⁻³. The most common fuel for gas turbines is natural gas⁴, which mainly consists of methane. Compared with flame combustion, the temperature needed for catalytic combustion of natural gas is lower, and this leads to a decrease the formation of thermal NO_x .

Perovskites, ABO_3 (B = Mn, Co, Fe), have been extensively studied due to higher catalytic activity for methane combustion and high thermal ability as compared to that of noble metals^{1,5}. However, the high calcination temperature of the prepared catalysts inevitably leads to large crystallite size and lower specific surface area (less than $5 \text{ m}^2/\text{g}$) of the catalysts⁶, limiting the potential applications of these materials. Therefore, new methods which yield perovskite-type catalysts with increased specific surface area are required.

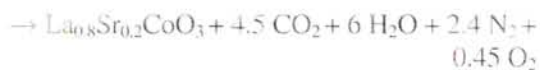
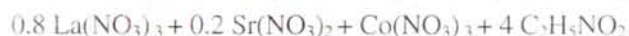
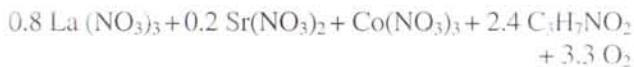
We report herein the synthesis of perovskite $\text{La}_{0.8}\text{Sr}_{0.2}\text{CoO}_3$ oxides prepared by solution combustion, with a view to boosting catalytic performance by enhancing specific surface area of the catalyst. The effects of organic fuels on the structure and the catalytic activities of $\text{La}_{0.8}\text{Sr}_{0.2}\text{CoO}_3$ mixed

oxides are also reported. The prepared samples have been characterized by XRD, IR, BET and TPR and have been used successfully for CH_4 combustion.

Materials and Methods

Preparation and characterisation of catalysts

Different organic fuels (*DL*-alanine, glycine or glycerol) were used to produce $\text{La}_{0.8}\text{Sr}_{0.2}\text{CoO}_3$ mixed oxides via SCS technique. Lanthanum, strontium and cobalt nitrates in the desired molar ratio were dissolved in deionized water with constant stirring. To this solution, organic fuel, *DL*-alanine (or glycine, glycerol), was added, keeping the organic fuel : cobalt nitrate mole ratio as 2.4:1 (or 4:1, 1.5:1). In addition to reacting with the precursors (i. e., metal nitrates), the organic fuels also form complexes with metal cations in aqueous solution. This ensures good solution homogeneity, ruling out preferential precipitation of ionic species. The overall combustion reactions can be written as follows:



The prepared aqueous solutions were transferred into a ceramic dish and placed into an oven, preheated at 450 °C. After water evaporation, the heat released in the fast reaction allowed the formation of the catalysts as powder. Then the powdered catalysts were calcined at 700 °C for 2 h. Finally, the synthesized $\text{La}_{0.8}\text{Sr}_{0.2}\text{CoO}_3$ catalysts were pulverized to *ca.* 60-80 mesh size.

Powder X-ray diffraction (XRD) data were obtained using an X-ray diffractometer (type D8/ADVANCE, Germany) over the range $20^\circ \leq 2\theta \leq 80^\circ$, at room temperature, operating at 40 kV and 30 mA, using Cu K α radiation combined with the nickel filter.

BET surface area and porous texture were evaluated by N_2 adsorption isotherms obtained at 77 K using an ASAP2020 (micrometrics) equipment. Before each measurement, the samples were degassed at 623 K in vacuum (0.13 Pa) for 1 h. The surface area was calculated with the BET equation.

The FT-IR spectra were recorded by a Nicolet 5700 Fourier transform instrument. The skeletal spectra in the region 1600- 400 cm^{-1} have been obtained with KBr pressed disks and a KBr beam splitter.

Temperature-programmed reduction (TPR) was carried out with an in-house apparatus over 0.1 g catalyst. Prior to TPR, the samples were pretreated at 700 °C for 2 h in air and cooled to room temperature. Then the pretreated samples were heated from room temperature to 700 °C in N_2 (35 ml/min) at a rate of 10 °C/min in order to remove any impurities. After cooling to room temperature under N_2 , a gas mixture consisting of H_2 and N_2 (5:95 v/v) was introduced into the system and heated at a rate of 10 °C/min for recording the TPR spectra.

Catalytic activity

The catalytic combustion experiments of methane were performed in a continuous microreactor by feeding a gaseous mixture of CH_4 (2 vol. %), O_2 (12.5 vol. %) and N_2 (rest) over 100 mg catalyst with 20000 h^{-1} GHSV and 350-650 °C reaction temperature. The gas composition was analysed before and after the reaction by an online gas chromatographic set up with thermal conductor detector (TCD), connected with a computer integrator system and Porapak Q column. The activity of the catalysts was measured as CH_4 conversion.

Results and Discussion

The X-ray diffraction patterns of $\text{La}_{0.8}\text{Sr}_{0.2}\text{CoO}_3$ mixed oxides are shown in Fig.1. The diffraction peaks are observed with 2θ values of 23.4, 33.3, 40.9,

47.8 and 59.4°, which correspond to (012), (110), (202), (024) and (214) planes of $\text{La}_{0.8}\text{Sr}_{0.2}\text{CoO}_3$ mixed oxides, respectively. The results of XRD clearly indicate that all the samples prepared by different organic fuels have the rhombohedral distorted perovskite structure.

The distortion of the active unit BO_6 is one of the important reasons for showing different activity. For the evaluation of average crystallite size and lattice distortion, Scherrer equation, $L=0.9\lambda/(\beta\cos\theta)$ and $\beta^2\cos^2\theta=4/\pi^2(\lambda/L)^2+32(\epsilon^2)\sin^2\theta$, were used. Here, L is the average crystallite size, λ , the X-ray wavelength (0.154nm), β , the half-peak width, θ , the diffraction angle and $(\epsilon^2)^{1/2}$, the lattice distortion in the direction of the (110) plane. The average crystallite size of the particles is in the range of 13-17 nm as determined by Scherrer's equation. Solution combustion synthesis is, therefore, effective for the preparation of nanosized materials of uniform composition. During solution combustion synthesis, the reactants are uniformly dispersed at the molecular level in the combustion mixture. When combustion occurs, the nucleation and growth of the particles take place only through short-distance diffusion of the nearby atoms. Due to the short life span of the combustion reaction, long distance diffusion of the atoms is not facilitated resulting in the formation of nanosized materials⁷. As compared with $\text{La}_{0.8}\text{Sr}_{0.2}\text{CoO}_3$ catalysts prepared by glycerol and glycine, the average crystallite size of $\text{La}_{0.8}\text{Sr}_{0.2}\text{CoO}_3$ catalyst prepared by DL-alanine is smaller, although the lattice distortion is greater

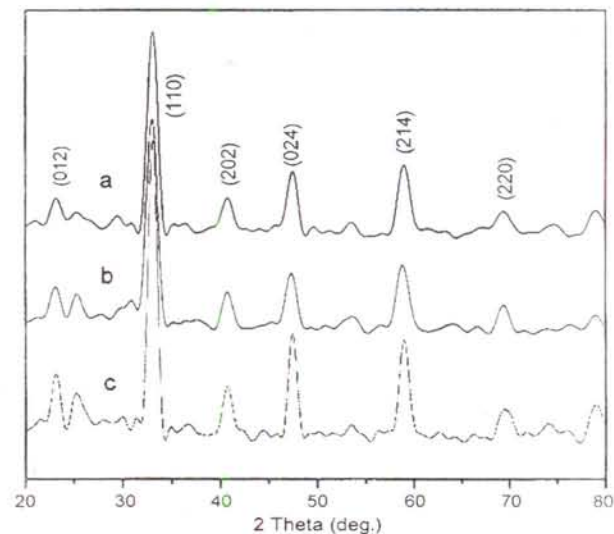


Fig. 1-XRD patterns of the $\text{La}_{0.8}\text{Sr}_{0.2}\text{CoO}_3$ catalysts prepared by SCS method. [a, alanine; b, glycerol; c, glycine].

(Table 1). The increase of lattice distortion increases the B-O₁ bond length and decrease B-O₁₁ bond length (O₁: oxygen in the c lattice axis; O₁₁: oxygen in x-y lattice plane). As a result, the mobility of O₁ will increase, which facilitates the process of oxidation reaction⁸⁻¹⁰.

BET surface area

N₂ adsorption-desorption isotherms of the La_{0.8}Sr_{0.2}CoO₃ catalysts prepared by SCS method were studied. All the isothermal results show hysteresis loops, which conform to a porous morphology. Such isothermal curves exhibit an intermediate profile between type B and D with a porous morphology, typical of lamella structure perforated by a large number of pores¹¹. On the other hand, the isothermal profiles of the samples show a slow increase at the relative pressure, $P/P_0 = 0.32-0.96$, which indicates that the samples have a broader pore-size distribution.

The BET data of the samples are presented in Table 1. For La_{0.8}Sr_{0.2}CoO₃ prepared by DL-alanine, glycerol and glycine, BET surface area decreases gradually. The resulting small particle sizes lead to

Organic fuel	T ₅₀ (°C)	T ₁₀₀ (°C)	Specific surface area (m ² /g)	Average crystallite size L ₍₁₁₀₎ (nm)	Lattice distortion (ε ²) ^{1/2} (10 ⁻³)
Alanine	470	550	20.31	13.04	4.58
Glycerol	485	560	19.01	14.56	4.46
Glycine	505	620	15.31	17.21	4.20

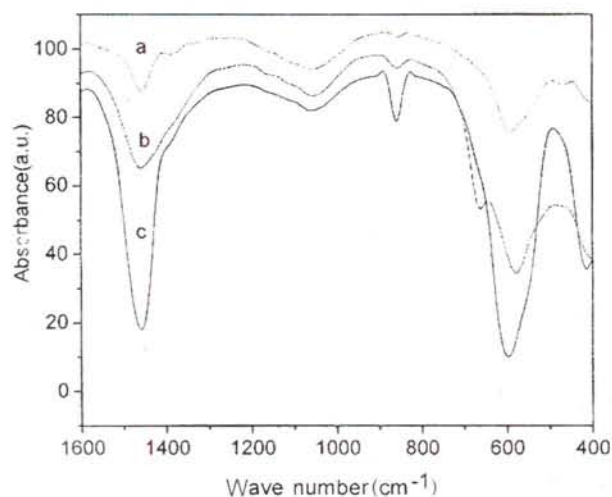


Fig. 2-IR spectra of the La_{0.8}Sr_{0.2}CoO₃ catalysts prepared by SCS method. [a, alanine; b, glycerol; c, glycine].

large BET surface areas (largest surface area is seen for the sample prepared with DL-alanine). The BET results show that the surface areas of the porous samples prepared by SCS method are much larger than those of the samples prepared via conventional synthesis routes¹² ($\leq 5-6 \text{ m}^2/\text{g}$), which is advantageous for the combustion reaction of methane.

FT-IR studies

The FT-IR spectra of the La_{0.8}Sr_{0.2}CoO₃ catalysts prepared by SCS method are shown in Fig. 2. All samples show two strong absorption bands about at 600 cm⁻¹ and 400 cm⁻¹, which may be attributed to Co-O stretching vibration ($\nu_{\text{Co-O}}$ mode) and O-Co-O deformation vibration ($\delta_{\text{O-Co-O}}$ mode), respectively. The vibration bands found here agree with the reported values for La_{0.8}Sr_{0.2}CoO₃ prepared by the sol-gel method using stearic acid¹³. The results of IR spectrum confirm that the perovskite phase is formed, which is in accordance with the XRD results.

H₂-TPR studies

The TPR profiles of the catalyst provide useful information about the reducibility of Co³⁺ species in the La_{0.8}Sr_{0.2}CoO₃ catalysts prepared by SCS method, since La³⁺ and Sr²⁺ of the A-site both are non-reducible under the condition of H₂-TPR. As shown in Fig. 3, there are two peaks (α and β) for all the catalysts, suggesting the occurrence of a multiple-step reduction. Conceivably, the partial substitution of La³⁺ by Sr²⁺ would result in increase in the

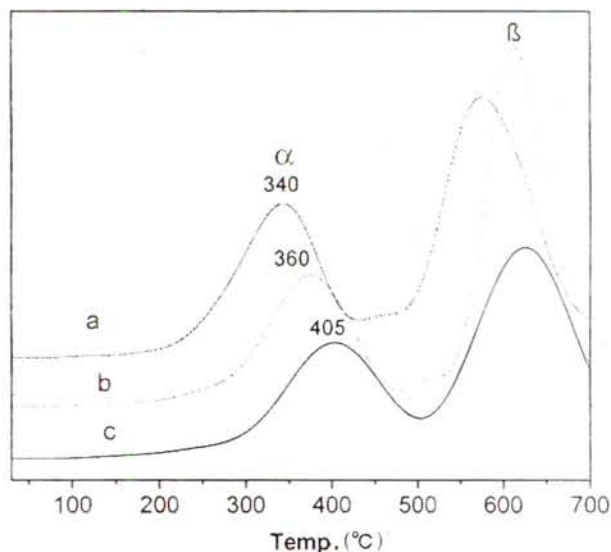
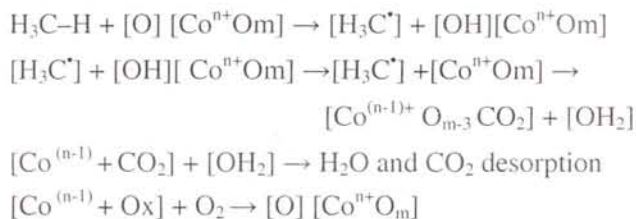


Fig. 3-H₂-TPR profiles of the La_{0.8}Sr_{0.2}CoO₃ catalysts prepared by SCS method. [a, alanine; b, glycerol; c, glycine].

concentration of Co^{3+} and oxygen vacancies due to charge compensation accomplished by oxidation from Co^{2+} to Co^{3+} and by the formation of an oxygen-deficient perovskite-type ABO_3 , which would lead to an increase in the reducibility. The peak α may be attributed to chemisorption oxygen and the partial reduction of Co^{3+} , i.e., $2\text{Co}^{3+} + \text{O}^{2-} + \text{H}_2 \rightarrow 2\text{Co}^{2+} + \text{H}_2\text{O}$, with the $\text{La}_{0.8}\text{Sr}_{0.2}\text{CoO}_3$ catalysts still preserved in the perovskite-type phase structure as a whole. The temperature of α -peak reflects binding capacity between the sample and oxygen. Most likely, peak β corresponds to the reduction of Co^{2+} to Co^0 , which leads to the breakdown of the perovskite-type phase. It may be seen that temperature of the α and β peaks of $\text{La}_{0.8}\text{Sr}_{0.2}\text{CoO}_3$ catalyst prepared by DL-alanine is lower than that of the catalyst prepared by glycine or glycerol, demonstrating that the activities of oxygen vacancies and lattice oxygen over the $\text{La}_{0.8}\text{Sr}_{0.2}\text{CoO}_3$ catalyst prepared by DL-alanine are the maximum, and the binding capacity between Co^{3+} and oxygen is lower. Thus, chemisorbed and lattice oxygen over the $\text{La}_{0.8}\text{Sr}_{0.2}\text{CoO}_3$ catalyst prepared by DL-alanine move easily, which is favorable to the methane combustion reaction of methane.

In view of the above data, catalytic combustion of methane may be considered to proceed via the following schematic steps^{14,15}:



In the first activation step, the initial C-H bond is broken, most probably homolytically. The initial step, typically the slowest or controlling step, is followed by a presumably faster reaction. This reaction, step 2, is apparently spillover type, or at least involves a movement of the methyl (alkyl) radical leading to the reaction with additional oxygen species favorably coordinated around a strong electron acceptor Co^{n+} . This step leads to surface bound carbon dioxide and water. In many cases, desorption of these products, (step 3), is comparatively slow, thereby inhibiting the overall rate of catalytic combustion. The presence of $[\text{Co}^{n+}\text{O}_m]$ seems essential for fast and complete oxidation with carbon dioxide and water as the only products. It is reasonable to consider octahedral coordination and (sufficiently) fast oxygen mobility

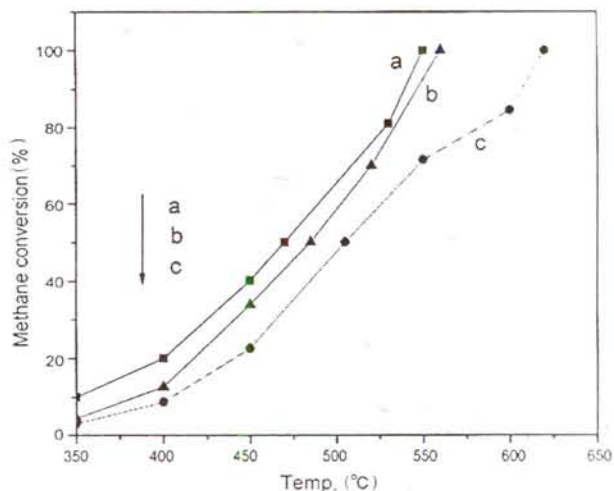


Fig. 4—Catalytic activity profiles of the $\text{La}_{0.8}\text{Sr}_{0.2}\text{CoO}_3$ catalysts prepared by SCS method. [a, alanine; b, glycerol; c, glycine].

as the critical characteristics. The overall kinetics will also depend on the availability of the reactive oxygen species, as expressed by the rate of step 4 (r_4). It is easy to understand that r_4 should be related to the overall oxygen mobility. In accordance with the schematic steps of catalytic methane combustion, we may conclude that the enhancement of oxygen mobility was favorable to methane combustion reaction.

Catalytic activity in methane combustion reaction

The catalytic activity of CH_4 combustion over the $\text{La}_{0.8}\text{Sr}_{0.2}\text{CoO}_3$ catalysts, prepared by SCS method, is shown in Fig. 4. Comparison of T_{50} , T_{100} and the conversion curves of CH_4 combustion shows that the organic fuels have a significant effect on the catalytic activity for CH_4 combustion. T_{50} and T_{100} of CH_4 combustion over $\text{La}_{0.8}\text{Sr}_{0.2}\text{CoO}_3$ catalyst prepared by DL-alanine are lower than those of the catalysts prepared by glycine or glycerol (Table 1), which indicates that catalytic activity of $\text{La}_{0.8}\text{Sr}_{0.2}\text{CoO}_3$ catalyst prepared by DL-alanine for CH_4 combustion is the highest. Influence of the three organic fuels on CH_4 combustion is in the order: alanine > glycerol > glycine. The catalytic oxidative activity of the $\text{La}_{0.8}\text{Sr}_{0.2}\text{CoO}_3$ is higher than that reported earlier^{11, 14-16}. This may be explained as due to the different effect of the fuels on the process. A carboxylic and an amine group in the alanine molecule would possess a different tendency to form complexes with metal cations. The transition metals are most effectively complexed by amine group, and this may be the reason for the more intense reaction occurring with DL-alanine. The

$\text{La}_{0.8}\text{Sr}_{0.2}\text{CoO}_3$ catalyst prepared by *DL*-alanine possesses higher catalytic activity for CH_4 combustion, which is strongly related to the higher surface area, activities of the oxygen and lattice distortion¹⁷.

Reaction kinetics

Methane combustion on metal oxides is known to follow a redox mechanism and a variety of kinetic models for this reaction exists¹⁸⁻²⁰. The models are based on either a Langmuir–Hinshelwood bimolecular type process, or on a Marsvan Krevelen type process, or are purely empirical. In general, the reaction rates are first order in methane, while the order in oxygen may vary, usually from zero to ~0.5. Although, the general equation for the oxidation–reduction model is relatively complex, for most catalysts this may be reduced to a simple first-order kinetic model:

$$r = kP_{\text{CH}_4} \quad \dots (1)$$

According to the Arrhenius equation, $k = Ae^{-E_a/RT}$, Eq. (1) can be written as follows:

$$r = -dp / dt = Ae^{-E_a/RT} p_{\text{CH}_4} \quad \dots (2)$$

where A is the pre-exponential factor, T is the reaction temperature in K, E_a is the apparent activation energy, and R is the gas constant.

On integration of Eq. (2), we obtain:

$$-\ln \frac{P_{\text{CH}_4}}{P_0} = Ae^{-E_a/RT} \cdot t + C \quad \dots (3)$$

Since the gas-space velocity and the catalyst quantity are the same in the reaction process, the time spent by the gas that passes through the catalyst bed should be the same. The total gas pressure being constant, for CH_4 conversion, $x = p_{\text{CH}_4} / p_0$. Logarithm of Eq. (3) gives Eq. 4.

$$\ln[-\ln(1-x)] = -E_a / RT + C \quad \dots (4)$$

From Eq. 4, the apparent activation energy of the CH_4 combustion reaction can be obtained from the slope ($-E_a/R$) of plot of $\ln[-\ln(1-x)]$ versus $1/T$.

The activation energy is an indicator of how difficult or easy it is for a reaction to progress and to what extent. Reaction speed is increased due to decrease in

Table 2—Apparent activation energy of the $\text{La}_{0.8}\text{Sr}_{0.2}\text{CoO}_3$ catalysts prepared by SCS method

Organic fuel	Apparent activation energy(kJ/mol)
Alanine	66.6
Glycerol	70.1
Glycine	80.3

the activation energy by the catalysts. The apparent activation energy of the studied catalysts prepared by SCS method is shown in Table 2. In comparison to catalysts prepared by glycine or glycerol, the apparent activation energy of the catalysts prepared by *DL*-alanine is lower by 3.5 and 13.7 kJ/mol, respectively. The lower the activation energy, the greater is the constant K , and faster is the reaction which agrees with the present experiment results.

Acknowledgement

This work was supported by the Doctor Degree Special Scientific Research Fund of Ministry of Education of P.R. China (Project 20040403001).

References

- Zwinkels M F M, Jaras S G, Menon P G & Griffin T A, *Catal Rev Sci Eng*, 26 (1993) 319.
- Pfefferle L D & Pfefferle W C, *Catal Rev Sci Eng*, 29 (1987) 219.
- Forzatti P, *Catal Today*, 83 (2003) 3.
- Carroni R, Schmidt V & Griffin T, *Catal Today*, 75 (2002) 287.
- Rossetti R & Forni L, *Appl Catal B*, 33 (2001) 345.
- Kingsley J J & Pedreson L R, *Mater Lett*, 18 (1993) 89.
- Rao G R, Mishra B G & Sahu H R, *Mater Lett*, 58 (2004) 3523.
- Gao L Z, Dong B L, Li X L & Wu Y, *J Fuel Chem Tec*, 22 (1994) 113.
- Qi X Z, Ma Z & Wang S W, *Chem Indust Eng*, 17 (2000) 358.
- Luo L T, Zhong H & Yang X M, *J Serb Chem Soc*, 69 (2004) 783.
- Wu Y H, Luo L T & Liu W, *J Chem Sci*, 119 (2007) 1.
- Kucharczyk B & Tylus W, *Catal Today*, 90 (2004) 121.
- Lal B, Raghunandan M K, Gupta M & Singh R N, *Int J Hydro Energy*, 30 (2005) 723.
- Kirchnerova J & Klvana D, *Catal Lett*, 67 (2000) 175.
- Klvana D, Kirchnerova J, Gauthier P & Delval J, *Can J Chem Eng*, 75 (1997) 509.
- Alifanti M, Kirchnerova J & Delmon B, *Appl Catal A*, 245 (2003) 231.
- Cho S J, Song K S, Ryu I S, Seo Y S, Ryoo M W & Kang S K, *Catal Lett*, 58 (1999) 63.
- Klvana D, Vaillancourt J, Kirchnerova J & Chauki J, *Appl Catal A*, 109 (1994) 181.
- Ladavos A K & Pomonis P J, *J Chem Soc*, 88 (1992) 2557.
- Saracco G, Geobaldo F & Baldi G, *Appl Catal B*, 20 (1999) 277.